Development 118, 1245-1254 (1993)
Printed in Great Britain © The Company of Biologists Limited 1993

Mutations affecting the cytoskeletal organization of syncytial *Drosophila* embryos

William Sullivan[1,2,*], Patrick Fogarty[1] and William Theurkauf[2,†]

[1]Department of Biology, Sinsheimer Laboratories, University of California, Santa Cruz, CA 95064, USA
[2]Department of Biochemistry and Biophysics, School of Medicine, University of California, San Francisco, CA 94143, USA

*Author for correspondence at address[1]
[†]Present address: Department of Biochemistry and Cell Biology, State University of New York at Stony Brook, Stony Brook, NY 11794-5215, USA

SUMMARY

Cytoplasmic organization, nuclear migration, and nuclear division in the early syncytial *Drosophila* embryo are all modulated by the cytoskeleton. In an attempt to identify genes involved in cytoskeletal functions, we have examined a collection of maternal-effect lethal mutations induced by single P-element transposition for those that cause defects in nuclear movement, organization, or morphology during the syncytial embryonic divisions. We describe three mutations, *grapes*, *scrambled*, and *nuclear-fallout*, which define three previously uncharacterized genes. Females homozygous for these mutations produce embryos that exhibit extensive mitotic division errors only after the nuclei migrate to the surface. Analysis of the microfilament and microtubule organization in embryos derived from these newly identified mutations reveal disruptions in the cortical cytoskeleton. Each of the three mutations disrupts the actin-based pseudocleavage furrows and the cellularization furrows in a distinct fashion. In addition to identifying new genes involved in cytoskeletal organization, these mutations provide insights into cytoskeletal function during early *Drosophila* embryogenesis.

Key words: *grapes, scrambled, nuclear-fallout, Drosophila,* maternal-effect lethal mutation, microtubule organization, actin

INTRODUCTION

The generation of order and asymmetry at the cytoplasmic level is fundamental to many basic cellular functions including mitosis, directed cell movement, and developmental processes such as axis specification. All of these events are largely dependent on the cytoskeleton, which is responsible for organizing the cytoplasm of eukaryotic cells. The problem of cytoplasmic organization is particularly acute during early embryogenesis in *Drosophila*: the initial divisions are syncytial and many of the nuclei undergo a precise program of movements leading to the formation of a highly regular blastoderm embryo.

The initial nuclear divisions of early *Drosophila* embryogenesis have been thoroughly studied (Rabinowitz, 1941; Sonnenblick, 1950; Turner and Mahowald, 1977; Zalokar and Erk, 1976; Foe and Alberts, 1983; Stafstrom and Staehelin, 1984; Minden et al., 1989). The *Drosophila* embryo undergoes 13 rapid (8-21 minutes) synchronous nuclear divisions without accompanying cytokinesis. The first eight nuclear divisions occur in the interior of the embryo. After these divisions, the nuclei embark along one of three different division programs. The majority of the nuclei migrate to the cortex during nuclear cycles 8, 9, and 10. By the end of nuclear cycle 10, these nuclei are positioned at the surface of the embryo just beneath the plasma membrane, where they undergo four synchronous divisions as a regularly spaced cortical monolayer. Cellularization occurs during interphase of nuclear cycle 14. A second nuclear division pathway involves a few nuclei that migrate ahead of the main body of nuclei and reach the posterior cortex during nuclear cycle 9. During cycle 10, these nuclei are surrounded by plasma membranes to form the pole cells, the precursors of the germ line. A third nuclear division program is exhibited by a group of nuclei that fail to migrate outward toward the cortex during nuclear cycle 8. These nuclei, known as the yolk nuclei, remain in the interior of the embryo and become polyploid.

The cortical cytoskeleton of the *Drosophila* embryo has been characterized through immunofluorescence analysis of fixed material (Warn et al., 1984; Warn et al., 1985; Karr and Alberts, 1986; Warn and Warn, 1986; Warn et al., 1987). In addition, the dynamics of the cortical cytoskeleton has been followed in living embryos by microinjecting fluorescently labeled actin and tubulin (Kellogg et al., 1988). The injection of fluorescently labeled histones provides a means of following chromosome behavior (Minden et al., 1989). During interphase, the cortical actin becomes organized in a cap between the plasma membrane and the nucleus. At this stage, microtubule networks, which originate from a centrosome pair located between the nucleus and the actin cap, radiate inwards to encompass each

nucleus. As the nuclei progress into mitosis, the centrosomes separate further and their microtubules form a bipolar mitotic spindle parallel to the cortex. In addition, the actin is redistributed to become associated with transient invaginations of the plasma membrane, called pseudocleavage furrows. These furrows surround each of the tightly packed mitotic spindles (Warn et al., 1984; Karr and Alberts, 1986). Recently, cytological, biochemical and genetic approaches have identified a number of proteins responsible for organizing the cortical cytoskeleton of the *Drosophila* embryo (for review see Fryberg and Goldstein, 1990; Schweisguth et al., 1991).

To identify genes involved in the formation and dynamics of embryonic cytoskeletal structures, we have screened for mutations that specifically disrupt the embryonic syncytial divisions. Our strategy was based on inhibitor studies that demonstrate that the organized divisions, migrations, and spacing of the nuclei in the syncytial embryo are highly dependent on maternally supplied cytoskeletal components (Zalokar and Erk, 1976; Foe and Alberts, 1983; Warn et al., 1987; Planques et al., 1991; Hatanaka and Okada, 1991). For instance, disrupting the cortical actin filaments with cytochalasin, results in nuclear fusions specifically during the cortical nuclear divisions (Zalokar and Erk, 1976; Theurkauf, unpublished observations). Irregularities in the organization and behavior of the early embryonic nuclei, therefore, are likely to serve as sensitive indicators of defects in these cytoskeletal components. These cytoskeletal inhibitor studies motivated a search for maternal-effect mutations with similar effects.

A number of genetic screens has generated a large collection of maternal-effect mutations (Bakken, 1973; Rice and Garen, 1975; Gans et al., 1975; Zalokar et al., 1975; Mohler, 1977; Schupbach and Weischaus, 1986; Perrimon et al., 1986; Erdelyi and Szabad, 1989; Schupbach and Weischaus, 1989; Perrimon et al., 1989; Szabad et al., 1989). With only a few exceptions (Zalokar et al., 1975), the nuclear phenotype of syncytial embryos derived from females homozgous for these maternal-effect mutations has been described. We have examined the syncytial nuclear phenotype in 44 recently isolated P-element induced maternal-effect lethal mutations. Our studies have identified a set of mutations that result in the production of embryos that exhibit abnormal nuclear behavior during the cortical divisions. However, prior to their migration to the cortex, the nuclei behave normally in these embryos. During the cortical divisions, the mutant embryos also display specific disruptions of their cortical microtubules and actin networks. We suggest that at least some of the members of this group of maternal-effect mutations disrupt genes that are specifically involved in the organization of the cortical cytoskeleton.

MATERIALS AND METHODS

Stocks

The laboratories of Y. N. Jan (U.C. San Francisco)and A. Spradling (Carnegie Institution of Washington) generously provided us with the female-sterile mutations described in this screen (Bier et al., 1989; Karpen and Spradling, submitted). Oregon-R was used as the wild-type stock. Other mutations and chromosomes are described by Lindsley and Zimm (1992). The *daughterless-abo-like (dal)* mutation has been previously described (Sandler, 1977; Sullivan, 1987; Sullivan et al., 1990). The stocks were maintained on a standard corn meal/molasses medium at 25°C.

Genetic analysis

Complementation analysis was performed by obtaining all combinations of transheterozygote females bearing the maternal-effect mutations of interest. 10 of these transheterozygote females were mated to 10 wild-type males for 5 days. After 5 days, the adult flies were removed. The number of adults eclosing prior to day seventeen was recorded for each of the matings.

Deficiency analysis was performed by crossing heterozygous mutant females to heterozygous deficiency males. The hatch rate of embryos derived from females bearing a copy of the mutation over a deficiency was determined. A set of deficiencies that resulted in no hatching when in combination with one of the maternal-effect mutations enabled us to map the mutations. The following deficiencies were used to map *grapes*: Df(2L)osp29, Df(2L)r10, Df(2L)H20, Df(2L)TW137, Df(2L)M-HS5, and Df(2L)TW50. The deficiencies Df(3L)vin5, Df(3L)vin7, Df(3L)Ly, Df(3L)fzGf3b, Df(3L)fzM21, and Df(3L)fzD21 were used to map *nuclear-fallout*. The deficiencies Df(2R)st1, Df(2R)PK78K, and Df(2R)42 were used to map *scrambled*.

Revertant analysis of our P-element induced maternal-effect mutations was performed according to the procedure described by Cooley et al. (1988).

Mapping of the P-element by in situ polytene hybridization was performed as described by Engels et al. (1986), using a probe from the P-lac Z vector (Karpen and Spradling, 1992).

Cellular analysis

The embryos used in our analysis were derived from either normal females, females homozygous for the maternal-effect mutation, or females bearing the maternal-effect mutation and a deficiency for the mutation. The embryos were fixed through a modification of the Mitchison and Sedat (1983) protocol (Theurkauf, 1992). Fixed embryos were double stained for actin and microtubules, using fluorescein-conjugated phalloidin and rhodamine-conjugated mouse anti-tubulin antibodies, as described elsewhere for ovaries (Theurkauf, 1992). Immunoflourescence with an anti-*Drosophila* sperm-tail antibody was used to assay for fertilization in early-arrested embryos (Karr, 1991).

Conventional fluorescence microscopy was performed using a Nikon Microphot FXA photoscope. Laser scanning confocal microscopy was performed using a Biorad MRC600 confocal imaging system installed on an Olympus IMT2 inverted microscope and a Nikon Optiphot photoscope. The lenses used included the Nikon 60× Planapo (1.4 numerical aperture (na)), the Nikon Plan 20 DIC (0.5 na), the Olympus S Plan Apo 60×, Oil (1.4 na), and the Olympus D Plan Apo 20×, UV. Oil (0.8 na).

RESULTS

Nuclear phenotypes of embryos derived from 76 female-sterile mutations

Of the 76 P-element induced female-sterile mutants that we examined, 44 laid morphologically normal eggs. To define the time in development that the nuclei arrested or when the first abnormalities in nuclear behavior occurred, we examined the morphology and distribution of the nuclei in 0- to 4-hour embryos derived from homozyous mutant mothers. 12 of the 44 maternal-effect mutations resulted in homozygous females producing embryos that developed normally through cellularization at nuclear cycle 14. These

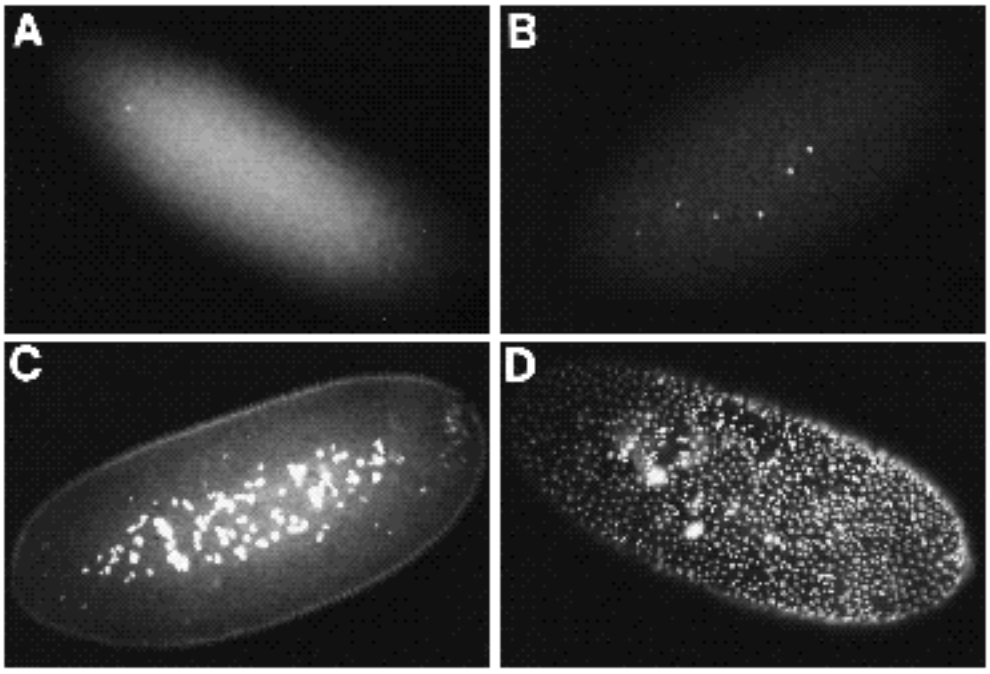

Fig. 1. Examples of typical nuclear phenotypes found in embryos derived from the maternal-effect mutations examined. (A) Nuclear-staining of an embryo derived from females homozygous for the maternal-effect mutation *fs25*. Females homozygous for this mutation consistently produce embryos that arrest during the first nuclear division. Double-staining with an anti-sperm tail antibody reveals that this embryo had been fertilized. The maternal-effect mutant *fs6* produces embryos that arrest at variable times during the premigration nuclear cycles (B). C depicts the maternal-effect mutation *fs4* in which the embryos consistently fail to produce pole cells. (D) Embryos derived from homozygous *fs37* females. The embryos undergo abnormal postmigration nuclear divisions and consequently possess unevenly sized and spaced cortical nuclei. Prior to nuclear migration, development is relatively normal in these embryos.

lines were not further characterized. Of the remaining 32 maternal-effect mutations, 23 caused severe disruptions or arrest of the nuclear divisions prior to the completion of nuclear migration at nuclear cycle 10 (Fig. 1). 2 of the 32 maternal-effect mutations, resulted in a failure of the embryos to form pole cells. These 2 mutations exhibited no other discernible nuclear defects (Fig. 1). Females homozygous for any of the remaining 7 maternal-effect mutations (*AS6034, AS5812, AS2257, AS742,* and *fs37* on chromosome two and *AS928* and *AS1479* on chromosome three) produced embryos that successfully completed nuclear migration, but underwent abnormal cortical nuclear divisions prior to cellularization (Fig. 1). Since this phenotype is similar to that observed in embryos treated with the specific actin-filament drug cytochalasin, these 7 mutations were therefore of particular interest and were subjected to the genetic and cell biological studies described below.

The maternal-effect mutations that preferentially disrupt the cortical blastoderm divisions represent at least four distinct loci

Complementation analysis of the two, third chromosome mutations, *AS928* and *AS1479*, demonstrates that they fall into a single complementation group. Deficiency analysis maps both mutations to region 70D2-70D6. *In situ* hybridization maps the P-element in *AS928* to region 70 and revertant analysis demonstrates the maternal effect is caused by the presence of a P-element. The complementation group defined by *AS928* and *AS1479* has been renamed *nuclear-fallout* (*nuf*). We designate these alleles nuf^1 and nuf^2 respectively.

Complementation analysis of the second chromosome mutations yields three complementation groups: *AS6034, AS5812,* and *AS2257* fall into a single complementation group, while *fs37* and *AS742* define the other two complementation groups. Deficiency analysis maps *AS6034, AS5812,* and *AS2257* to region 36A8-36D1. This genetic mapping is supported by in situ polytene hybridizations, which localizes the P-element to region 36A-36B in the *AS6034* stock. Revertant analysis confirmed that the maternal-effect in *AS6034* was caused by the presence of a P-element. The complementation group defined by *AS6034, AS5812,* and *AS2257* has been renamed *grapes* (*grp*). We designate these alleles grp^1, grp^2 and grp^3 respectively.

Deficiency analysis maps *fs37* to region 43B1-43E and in situ hybridization localizes the P-element to region 43. Revertant analysis of *fs37* demonstrates that the maternal effect is caused by the presence of a P-element. *fs37* has been renamed *scrambled* (*sced*).

AS742 was previously named *fsry9* and is a P-element induced allele of *staufen* (cytological position 55A; St. Johnson et al., 1991). Although the division defects observed in AS742-derived embryos are consistent and specific to the cortical divisions, the defects are not as extensive as observed in the other mutations in this set (Fig. 2). In addition, we do not know whether these defects are a direct consequence of the P-induced mutation. In this paper, we do not further analyze this mutation.

grp, *sced*, and *nuf* are therefore maternal-effect genes that preferentially disrupt the cortical nuclear divisions. For *sced*, grp^1, nuf^1, we observed the same phenotype whether the embryos were derived from females homozygous or hemizygous for these mutations. Although further analysis is required, this suggests that these mutations represent amorphic alleles.

As this screen was restricted to a relatively small number

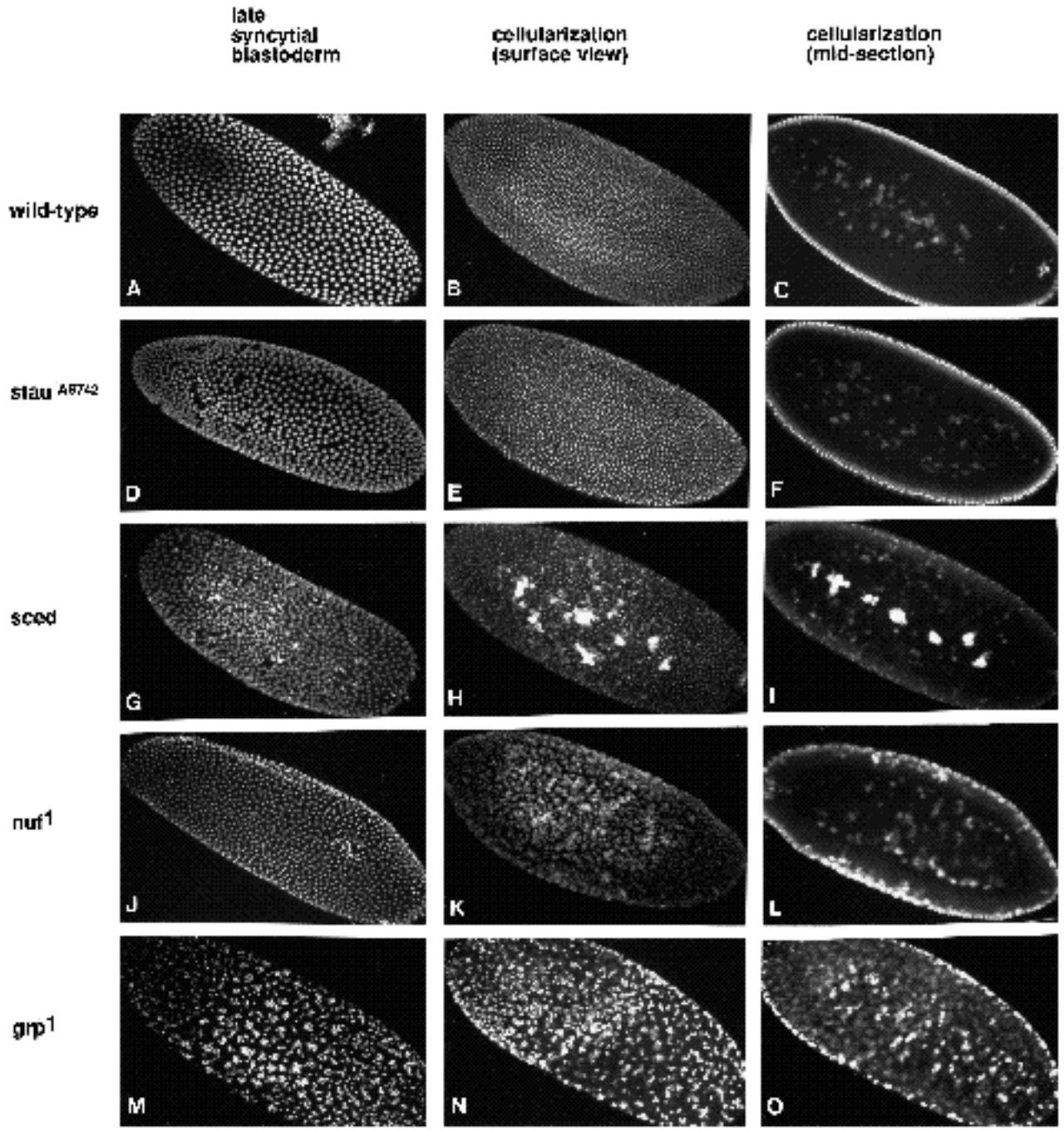

Fig. 2. 0- to 4-hour embryos derived from wild-type, *AS742* (designated *stau*^{AS742} see text), *sced*, *nuf*^{1}, and *grp*^{1} females were fixed with formaldehyde and stained with an anti-histone antibody. Each row, depicting embryos derived from one of these maternal-effect mutations, presents a surface view of a late syncytial blastoderm stage embryo (nuclear cycle 12 or 13), and a surface and cross sectional view of a cellularized embryo.

of available P-element-induced maternal-effect lethals, and did not include X chromosome mutations, it is clear that we have not saturated the genome for this class of maternal-effect mutations. For example, a previously characterized second chromosome maternal-effect mutation, *daughter -less-abo-like* (cytological region 32A-F), produces a preferential disruption of the cortical nuclear divisions, but was not recovered in this screen (Sandler, 1977; Sullivan et al., 1990).

Embryos derived from females homozygous for *grapes*, *scrambled*, or *nuclear-fallout* exhibit extensive nuclear division abnormalities only after the nuclei have migrated to the cortex

Initial observations indicated that *grp*^{1}, *nuf*^{1} and *sced* develop normally prior to the cortical divisions. To quantify these observations, we measured both the spacing and nuclear division synchrony in premigration embryos (nuclear cycles 5 through 8) derived from mothers homozy-

Table 1. Nuclear divisions in embryos from mothers homozygous for each of the maternal-effect mutations

		Nuclear cycle			
		5-8	9-10	11-14	No. of embryos
wild-type	Normal	39	34	49	
	Abnormal	2(5%)	1(3%)	1(2%)	126
sced	Normal	18	18	6	
	Abnormal	1(5%)	7(28%)	211(97%)	261
grp^1	Normal	49	45	8	
	Abnormal	1(2%)	2(4%)	60(88%)	165
nuf^1	Normal	48	33	16	
	Abnormal	3(6%)	0(0%)	102(86%)	202

Embryos derived from females homozygous for each of the maternal-effect mutations listed above were fixed with formaldehyde and their nuclei DAPI-stained. The nuclear phenotype of these embryos were scored with respect to their nuclear cycle. For nuclear cycles 5-8, an embryo was scored as abnormal if more than 2% of the nuclei were spaced less than 3 μm from their nearest neighbor or were greater than a half-nuclear cycle out of division synchrony with respect to their neighboring nuclei. For nuclear cycles 9-10, the same scoring scheme was employed. For nuclear cycles 11-13, an embryo was scored as abnormal if greater than 2% of its nuclei exhibited abnormal size or shape or had moved into the interior of the embryo. Estimates of the number of nuclei that had been removed from the cortical nuclear monolayer could be obtained by scoring the nuclei in the cortex of the embryo (within 10 μm of the plasma membrane) but beneath the surface monolayer of nuclei.

gous for each of these maternal-effect mutations. If greater than 2% of the nuclei of an embryo exhibited abnormal spacing or were greater than a half-nuclear cycle out of division synchrony with respect to their neighboring nuclei, the embryo was scored as abnormal. By this test, 5% of wild-type embryos between nuclear cycles 5 and 8 were scored as abnormal (Table 1). Embryos derived from the three maternal-effect mutations exhibit values indistinguishable from the wild-type values. Thus, embryos derived from females homozygous for these maternal-effect mutations appear to develop normally prior to nuclear migration.

This assay was also used to examine nuclear cycles 9 and 10. Approximately 3% of the embryos derived from wild-type females were abnormal during these nuclear cycles. With the exception of *sced*-derived embryos, all of the mutants produced less than 10% abnormal embryos during nuclear cycles 9 and 10 (Table 1). In about 50% of the *sced* -derived embryos, uneven nuclear migration to the cortex was also observed.

In embryos derived from females homozygous for the maternal-effect mutations, extensive division irregularities occur during the postmigration cortical divisions (nuclear cycles 11-14). In these mutants, the cortical nuclei share the following abnormal features.

(1) Nuclei vary in size and shape, suggesting nuclear fusion events, division failures and other division abnormalities.

(2) Patches of nuclei differ in density and/or stage in the nuclear cycle from that of their neighboring nuclei.

(3) Regions of the cortex are free of nuclei; these regions often contain high concentrations of centrosomes.

(4) Nuclei are present in the cortical cytoplasm beneath the normal monolayer of cortical nuclei; often there is a visible increase in the number of nuclei in the interior of the embryo.

(5) Cellularization occurs at a reduced nuclear density, and the size of the nuclei and cells at cellularization are proportionally increased as the cellular density is decreased.

To quantify these observations, we estimated the percentage of nuclei in each postmigration embryo that were abnormally shaped, sized, or had moved into the interior of the embryo. If this was greater than 2%, the embryo was scored as abnormal. The results of this analysis are summarized in Table 1. For the embryos derived from the maternal-effect mutants, the percentage of embryos scored as abnormal during nuclear cycles 11-14 ranged from 83% to 98% compared with 2% for normal embryos.

The postmigration nuclear phenotypes typical of embryos derived from wild-type females and females homozygous for the maternal-effect mutations are documented in Fig. 2. The first column depicts a late syncytial blastoderm embryo derived from each of these lines. In comparison with the wild-type embryo (Fig. 2A), the embryos derived from the maternal-effect mutations exhibit irregular nuclear distributions, clumping of nuclei, and large gaps in the surface monolayer of nuclei (Fig. 2D,G,J,M). Previous studies suggest that these phenotypes are the consequences of abnormal cortical nuclear divisions (Sullivan et al., 1990).

The second and third columns of Fig. 2 show surface and cross sectional views, respectively, of the nuclear phenotype at cellularization (or the equivalent time in development) of embryos derived from these mutant females. Fig. 2B,C shows a normal embryo cellularized at nuclear cycle 14. The mutant embryos are ordered by an increasing severity of cellularization defects. Embryos derived from *sced* females cellularize with fewer cortical nuclei and an excess of interior nuclei (Fig. 2H,I). This is probably a consequence of cortical division errors and the subsequent loss of abnormal nuclei from the surface monolayer (Minden et al., 1989; Sullivan et al., 1990) In addition, the distribution of cortical nuclei is irregular in *sced*-derived embryos (Fig. 2H). Embryos derived from *nuf^1* females also cellularize with fewer surface nuclei and a corresponding increase of interior nuclei (Fig. 2K,L). In *nuf^1*-derived embryos, the distribution of surface nuclei during cellularization is extremely irregular. The nuclei often form clusters of varying size and shape (Fig. 2K). Finally, embryos derived from *grp^1* females do not cellularize (Fig. 2N,O). Nomarski images reveal that they fail even to initiate cellularization. As the cortical divisions progress, the nuclei clump into clusters of approximately 5-25 nuclei (Fig. 2M,N). *grp^1* differs from the other mutations in that a much smaller proportion of the abnormal nuclei move into the interior of the embryo.

sced, *nuf*, and *dal* mutants develop distinct defects in the cortical cytoskeleton

This set of maternal-effect mutations all produce extensive mitotic division errors only after the nuclei have migrated to the cortex. Although they share this phenotype, analysis of the cytoskeleton indicates that at least three of these mutations produce distinct disruptions in embryonic actin and tubulin organization during the cortical divisions. Fig. 3 depicts the actin and microtubule organization of syncytial and cellularized embryos derived from wild-type, *dal*, *nuf^1*

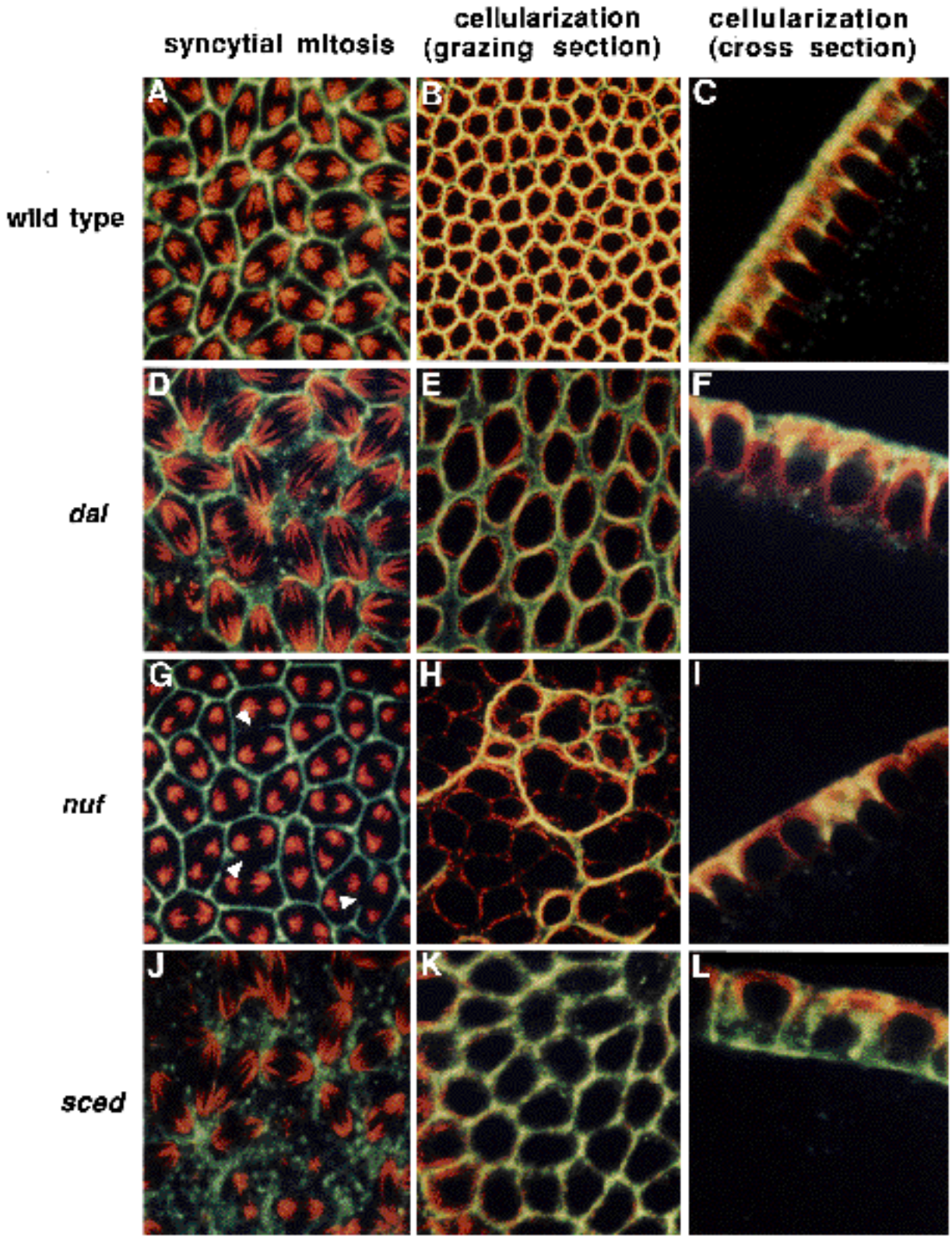

Fig. 3. Confocal images of formaldehyde-fixed embryos derived from wild-type, *dal*, *nuf*^{1} and *sced* females that have been stained for both actin (yellow/green) and tubulin (red). The top row depicts a surface view of a normal embryo in metaphase during the cortical divisions (A), a surface view (B) and a cross sectional view (C) of a cellularized wild-type embryo. The remaining rows depict equivalent views of embryos derived from the maternal-effect mutations. As described more fully in the text, this analysis indicates that each of the mutations disrupts the cortical cytoskeleton in a distinct fashion.

and *sced* mutant females. *grp*-derived embryos have not been included in this analysis because they arrest prior to cellularization. The first column in Fig. 3 presents a surface view of metaphase embryos during the cortical divisions. The second and third columns depict surface and cross-sectional views, respectively, of the embryos during cellularization at nuclear cycle 14.

dal, *nuf*, and *sced* all produce defects in the pseudocleavage furrows. In wild-type embryos, the actin-based pseudocleavage furrows completely encircle each of the metaphase spindle complexes during the syncytial cortical divisions (Fig. 3). Similar views of *dal*-derived embryos reveal fused and unevenly spaced spindles (Fig. 3D). Previous analysis indicates that these spindle defects are a consequence of incomplete centrosome separation during the previous interphase (Sullivan et al., 1990). In *dal*-derived embryos, abnormal pseudocleavage furrows are associated with defective spindles, while normal spindles are surrounded by normal furrows (Fig. 3D). The defects in actin organization in *dal* embryos therefore appear to be a consequence of the centrosome migration defect and subsequent abnormalities in spindle distribution. The formation of actin caps during interphase appears normal in *dal*-derived embryos.

Fig. 3G depicts a similar view of a nuf^1-derived embryo. The first obvious defect occurs during nuclear cycle 12 with the appearance of large gaps in the actin-based furrows surrounding each spindle (see arrow, Fig. 3G). Interestingly, the gaps usually appear in regions of the furrow that are closest to the metaphase plate. In spite of the defective furrows, the spacing and structure of the spindles appear normal. Thus, unlike *dal*, the first observable defect occurs in the actin-based pseudocleavage furrows rather than in the microtubules or microtubule-associated structures such as the centrosomes. In nuf^1-derived embryos, the formation of the actin-caps during interphase occurs normally. During the later cycles, fused and unequally spaced spindles become apparent in these mutant embryos.

In *sced*-derived embryos, there is an almost complete failure in pseudocleavage furrow formation (Fig. 3J). During nuclear cycle 10, in *sced*-derived embryos, the mitotic actin structures are severely disrupted, although observable defects in the mitotic spindles are infrequent. Later, defective spindles are seen. Because the actin defects precede spindle defects in *sced*-derived embryos, the spindle abnormalities in these embryos are likely to be a consequence of failed furrow formation, rather than a cause. As with *dal* and *nuf*, the *sced* mutation does not block formation of the interphase actin caps (Theurkauf, Sullivan, and B. Alberts, unpublished data).

The above analysis demonstrates that *sced*, nuf^1 and *dal* embryos can be distinguished by the nature of their cytoskeletal defects during the syncytial blastoderm divisions. Analysis of actin and microtubule organization demonstrates that these mutations also produce distinct defects during cellularization. An optical section of a cellularized wild-type embryo at nuclear cycle 14 reveals evenly spaced nuclei surrounded by microtubules which in turn are surrounded by a ring of actin (Fig. 3B). The actin filaments are just beneath the plasma membrane and the microtubules are tightly associated with each nucleus. During cellularization, the nuclei elongate perpendicularly to the plasma membrane. In the cross-sectional views, the tightly associated microtubules outline the elongated nuclei (Fig. 3C).

In *dal*-derived embryos, microtubule and actin organization during nuclear elongation and membrane invagination appear normal (Fig. 3E,F), although these embryos cellularize with enlarged nuclei at one-half of the normal density (Sullivan et al., 1987). Therefore the *dal*-induced defect is likely to be specific to the syncytial divisions and does not affect the process of cellularization.

While cellularization occurs in *sced*-derived embryos, neither the honeycomb actin pattern nor the ring of microtubules outlining each of the cellularized nuclei is as distinct as observed in wild-type embryos (Fig. 3K,L). The cross sectional view reveals that nuclear elongation is disrupted and that the microtubules are not closely associated with the nuclei in cellularized *sced*-derived embryos (Fig. 3L). As with *dal*, the nuclei and cells are larger and at a lower density relative to wild-type nuclei. This is likely to be the result of the products of the abnormal cortical divisions moving into the interior of the embryo, which leaves fewer, larger surface nuclei.

The cellularization phenotype of nuf^1-derived embryos is dramatically different from either *dal* or *sced*. As panels H and I illustrate, distinct cellularization furrows occur in nuf^1 embryos, but the pattern is irregular with groups of nuclei being encompassed by a single cellularization furrow. Unlike *sced*, distinct rings of microtubules do form around each nucleus during cellularization, and this occurs whether or not membrane invagination has occurred. The microtubules remain tightly associated with each nucleus and nuclear elongation appears to occur normally.

DISCUSSION

In an attempt to identify genes involved in the organization of the cytoskeleton of syncytial *Drosophila* embryos, we have initiated a cytological screen of embryos derived from females homozygous for maternal-effect lethal mutations. This analysis has led to the identification of a class of mutations in which the females produce embryos that develop normally until the nuclei migrate to the cortex. However, once the nuclei reach the cortex, these embryos acquire abnormal mitotic figures, irregularly shaped nuclei, and uneven nuclear spacing.

There are a number of possible explanations for the stage-specific phenotypes found in this class. These mutations could be hypomorphic alleles of genes required during both the premigration and postmigration divisions, but the level or activity of the mutant gene product may be such that it is used up at the time the nuclei reach the cortex. We do not believe that this is the case, however, because the transition from normal to abnormal divisions is rather abrupt, occurring only after the nuclei reach the cortex. With hypomorphic alleles one might expect more variation in the timing of the abnormal divisions. In addition, for *sced*, nuf^1 and grp^1, the same phenotype is observed whether the embryos are derived from females homozygous or hemizygous for the mutation.

We believe that these mutations are likely to disrupt genes whose products are specifically involved in the organization

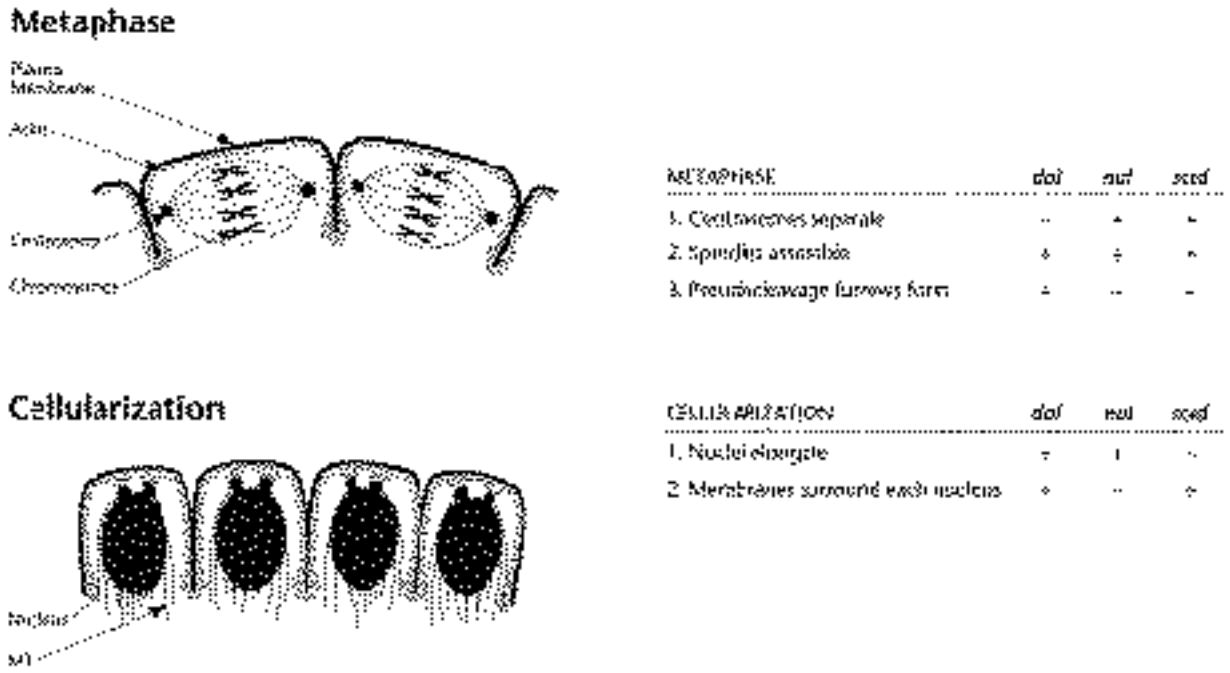

METAPHASE	*dal*	*nuf*	*sced*
1. Centrosomes separate	–	+	+
2. Spindle assembles	+	+	+
3. Pseudocleavage furrows form	+	–	–

CELLULARIZATION	*dal*	*nuf*	*sced*
1. Nuclei elongate	+	+	+
2. Membranes surround each nucleus	+	–	+

Fig. 4. This figure summarizes our analysis of the cortical cytoskeleton in *dal, sced,* and *nuf* derived embryos. A '+' indicates that the event occurs normally while a '−' indicates that the event does not occur or occurs abnormally. The two tables indicate that although each of these mutations exhibit similar nuclear defects, they exhibit distinct cellular defects. Each mutation appears to be disrupting a different step in the process of pseudocleavage furrow formation and cellularization.

of the cortical cytoskeleton. As described, the dividing nuclei induce the formation of actin-based pseudocleavage furrows which are unique to the syncytial cortical divisions. Unlike normal cleavage furrows, these structures encompass each metaphase spindle. Previous studies suggest that they function as barriers to prevent improper connections between spindles and to prevent the nuclei from colliding with one another (Sullivan et al., 1990; Postner et al., 1992). It is likely that pseudocleavage furrow formation requires specialized proteins. The predicted effect on the nuclear behavior of a mutation that is disrupted in one of these proteins would be similar to that observed in the mutations described above. Studies of permeabilized embryos treated with the actin disrupting drug cytochalasin support this notion. This treatment results in a phenocopy of the mutations described above; embryos exhibit abnormal nuclear divisions only after the nuclei have migrated to the surface (Zalokar and Erk, 1976; Theurkauf, unpublished observation). Indeed, the cytological analysis of actin and microtubule organization in *sced* and *nuf*[1] embryos demonstrates that both of these mutations produce a specific defect in the actin-containing pseudocleavage furrows (Fig. 4).

The mutations described here support studies demonstrating that the cytoskeletal rearrangements of the cortical syncytial divisions and of cellularization involve both distinct and common elements. The previously described maternal-effect mutation *sponge* results in failed actin-cap and pseudocleavage furrow formation during the syncytial divisions (Postner et al., 1992). Surprisingly, during nuclear cycle 14, *sponge*-derived embryos form regular cellularization actin networks. Similarly, in *dal*-derived embryos, cellularization occurs normally even though the pseudocleavage furrows are disrupted as a result of failed centrosome separation during the syncytial divisions (Sullivan et al., 1990). The newly identified *sced* mutation dramatically disrupts the formation of the pseudocleavage furrows but has surprisingly little effect on the formation of the actin networks at cellularization. These three maternal-effect mutations define components or processes that preferentially disrupt actin dynamics during the syncytial divisions and do not appear to be significantly involved in the formation of the actin-based cellularization furrows.

Conversely, exhaustive deficiency screens have identified a small set of zygotic genes specifically involved in cellularization (Wieschaus and Sweeton, 1988; Merrill et al., 1988). Deficiencies for these genes do not disrupt the cytoskeletal or nuclear dynamics of the syncytial divisions. *serendipity alpha* and *nullo,* two of the genes specifically involved in cellularization, have been particularly well studied. Deficiencies for *serendipity alpha* result in gross disruptions of the actin/myosin network during cellularization. *serendipity alpha* codes for a 58×10^3 M_r protein that colocalizes with F-actin and is associated with the leading front of the invaginating plasma membrane during cellularization at nuclear cycle 14 (Schweisguth et al., 1990). By germband extension the protein is no longer present indicating that it is specifically involved in cellularization. Careful analysis of the *nullo* phenotype, reveals that *nullo* is involved in stabilizing the actin contractile network during cellularization, but it is not involved in the initial formation of this network (Simpson and Wieschaus, 1990). As expected, the *nullo* gene is also transiently expressed just prior to cellularization (Rose and Wieschaus, 1992).

In contrast to the genes described above, the phenotype of *nuf*- derived embryos suggests that this gene plays a similar role both in pseudocleavage furrow formation and

cellularization. In both cases, the actin-based furrows are capable of forming properly, but there are extensive gaps in the overall furrow network. The distribution of furrows during the syncytial divisions and the distribution of membrane invaginations during cellularization therefore both rely on normal *nuf* activity. These studies reveal that some gene products are required during the cortical syncytial divisions and cellularization while others are specifically required for one of these processes.

The similarity of the *nuf* phenotype to the zygotic mutations *nullo* and *serendipity* is striking (Simpson and Wieschaus, 1990; Schweisguth et al., 1990). In all three mutations, the cellularization furrows fail to encompass every nucleus creating an embryo with multinucleate cells. From the analysis of these zygotic cellularization mutations and extensive deficiency screening, it has been suggested that the syncytial divisions and even the initial formation of the actin/myosin contractile network at cellularization are maternally controlled while the zygotic genes function to stabilize the cellularization furrows (Simpson and Wieschaus, 1990). Possibly *nuf* provides a maternally supplied component required for pseudocleavage furrow formation during the syncytial divisions and also the initiation of furrow formation at cellularization. This predicts that, unlike *nullo*, the initial formation of the cellularization furrows would be perturbed in *nuf*-derived embryos. Although preliminary analysis supports this interpretation, a conclusion must await more extensive phentoypic analysis. Although there are a number of possibilities concerning the relationship of *nuf*, *serendipity* and *nullo*, an attractive working model is that the maternally supplied *nuf* acts upstream and in concert with the zygotic genes *serendipity* and *nullo* to form and stabilize the actin networks during cellularization.

In the zygotic mutation *pebbles*, pseudocleavage furrow formation and cellularization are not disrupted, but cytokinesis fails during the division following cellularization (Hime and Saint, 1992). Therefore, the three similar actin-mediated events of *Drosophila* embryogenesis, pseudocleavage furrow formation, cellularization, and cytokinesis each require unique gene products.

The *sced* and *nuf* mutations also define dependency relationships during formation of the pseudocleavage furrows and during cellularization. It is evident from the *sced* phenotype that the formation of the spindles is independent of pseudocleavage formation. In addition, the *sced* cellularization phenotype demonstrates that cellularization is independent of nuclear shaping and the proper close association of microtubules with each nucleus. In *nuf*-derived embryos, microtubules properly encompass each nucleus even in the absence of the actin-based plasma membrane at cellularization. This cellularization phenotype demonstrates that microtubule alignment around the nucleus during cellularization is independent of the cellularization furrows.

Although each of the maternal effect mutations described in this paper produces a distinct disruption in the cortical cytoskeleton, they cause a number of common nuclear phenotypes, including a deficiency of cortical nuclei and excess interior nuclei at the time of cellularization. The excess interior nuclei are explained by previous studies demonstrating that the products of abnormal cortical divisions move into the interior of the embryo, leaving fewer cortical nuclei (Minden et al., 1989, Sullivan et al., 1990). The newly identified mutations demonstrate that the removal of abnormal nuclear products into the interior of the embryo is a general response of the *Drosophila* embryo. In addition, previous studies have demonstrated that when the abnormal nuclei move into the interior they leave their centrosomes on the surface. We have found that this is also true for the mutations described here (data not shown).

Recently, a large number of actin and tubulin-associated proteins have been isolated from the early *Drosophila* embryo (Miller et al., 1989; Kellogg et al., 1989). Immunofluorescence has revealed that some of these proteins are specifically located in the cortex of the embryo. We believe the mutational analysis described in our studies provides a complimentary functional approach towards identifying cortical cytoskeletal-associated proteins of the *Drosophila* embryo. In addition to a molecular characterization of these mutations, we are also initiating studies of the microtubule and microfilament dynamics in embryos derived from females homozygous for these mutations.

We would like to thank Bruce Alberts, Douglas Kellogg, Jordan Raff, and John Tamkun for their critical reading of this manuscript. We would especially like to thank Dr. Bruce Alberts in whose laboratory a significant portion of this work was performed. We also thank Tim Karr for kindly supplying us with the *Drosophila* anti-sperm tail antibody. Finally we express our appreciation to the Y.N. Jan and the A. Spradling laboratories for generously providing us with the maternal-effect mutations.

This work was supported by grants to W. Sullivan from the National Institutes of Health (R29 GM46409-01) and the American Cancer Society (JFRA-366) and to W. E. Theurkauf from the Damon Runyon-Walter Winchell Cancer Research Fund (DRG-945) and to Bruce M. Alberts from the National Institutes of Health (R01 GM23928 and P01 GM31286).

REFERENCES

Bakken, A. H. (1973). A cytological and genetic study of oogenesis in *Drosophila melanogaster*. *Dev. Biol.* **33**, 100-122.

Bier, E., Vaessin, H., Shepherd, S., Lee, K., McCall, S., Barbel, S., Ackerman, L., Carretto, R., Uemura, T., Grell, E., Jan, L. Y. and Jan Y. N. (1989). Searching for pattern and mutation in the *Drosophila* genome with a P-lacZ vector. *Genes Dev.* **3**, 1273-1287.

Cooley, L., Kelley, R. and Spradling, A. (1988). Insertional mutagenesis of the *Drosophila* genome with single P elements. *Science* **239**, 1121-1128.

Engels, W. R., Preston, C. R., Thompson, P. and Eggleston, W. B. (1986). In situ hybridization to *Drosophila* salivary chromosomes with biotinylated probes and alkaline phosphatase. *Focus* **8**, 6-8.

Erdelyi, M. and Szabad, J. (1989). Isolation and characterization of dominant female sterile mutations of *Drosophila melanogaster*. I. Mutations on the third chromosome. *Genetics* **122**, 111-127.

Foe, V. E. and Alberts, B. M. (1983). Studies of nuclear and cytoplasmic behavior during the five mitotic cycles that precede gastrulation in *Drosophila* embryogenesis. *J. Cell Sci.* **61**, 31-70.

Fryberg, E. A. and Goldstein, L. S. B. (1990). The *Drosophila* cytoskeleton. *Ann. Rev. Cell Biol.* **6**, 559-596.

Gans, M., Audit, C. and Masson, M. (1975). Isolation and characterization of sex-linked female sterile mutants in *Drosophila melanogaster*. *Genetics* **81**, 683-704.

Hatanaka, K. and Okada, M. (1991). Retarded nuclear migration in *Drosophila* embryos with aberrant F-actin reorganization caused by maternal mutations and by cytochalasin treatment. *Development* **111**, 909-920.

Hime, G. and Saint, R. (1992). Zygotic expression of the pebble locus is required for cytokinesis during the postblastoderm mitoses of *Drosophila*. *Development* **114**, 165-171

Karpen, G. H. and Spradling, A. C. (1992). Analysis of subtelomeric heterochromatin in the *Drosophila* minichromosome Dp1187 by single P-element insertional mutagenesis. *Genetics* **132**, 737-757

Karr, T. L. and Alberts, B. M. (1986). Organization of the cytoskeleton in early *Drosophila* embryos. *J. Cell Biol.* **102**, 1494-1509.

Karr, T. L. (1991). Intracellular sperm/egg interactions in Drosophila: A three-dimensional structural analysis of a paternal product in the developing egg. *Mech. Dev.* **34**, 101-111.

Kellogg, D. R., Mitchison, T. J. and Alberts, B. M. (1988). Behavior of microtubules and actin filaments in living *Drosophila* embryos. *Development* **103**, 675-686.

Kellogg, D. R., Field, C. M. and Alberts, B. M. (1989). Identification of microtubule-associated proteins in the centrosome, spindle, and kinetochore of the early Drosophila embryo. *J. Cell Biol.* **109**, 2977-2991.

Lindsley, D. L. and Zimm, G. G. (1992). *The genome of* Drosophila melanogaster. London, New York: Academic Press, Inc.

Merrill, P. T., Sweeton, D. and Wieschaus, E. (1988). Requirements for autosomal gene activity during precellular stages of *Drosophila melanogaster*. *Development* **104**, 495-509.

Miller, K., Field, C. M. and Alberts, B. M. (1989). Actin binding proteins from Drosophila embryos: a complex network of interacting proteins detected by F-actin affinity chromatography. *J. Cell Biol.* **109**, 2963-2975

Minden, J. S., Agard, D. A., Sedat, J. W. and Alberts, B. M. (1989). Direct cell lineage analysis in *Drosophila melanogaster* by time lapse three dimensional optical microscopy of living embryos. *J. Cell Biol.* **109**, 505-516.

Mitchison, T. J. and Sedat, J. W. (1983). Localization of antigenic determinants in whole *Drosophila* embryos. *Dev. Biol.* **99**, 261-264.

Mohler, J. D. (1977). Developmental genetics of the *Drosophila* egg I. Identification of 59 sex-linked cistrons with maternal-effects on embryonic development. *Genetics* 259-272.

Perrimon, N., Mohler, D., Engstrom, L. and Mahowald, A. P. (1986). X-linked female-sterile loci in *Drosophila melanogaster*. *Genetics* **113**, 695-712.

Perrimon, N., Engstrom, L. and Mahowald, A. P. (1989). Zygotic lethals with specific maternal-effect phenotypes in *Drosophila melanogaster*. I. Loci on the X chromosome. *Genetics* **121**, 333-352.

Planques, V., Warn, A. and Warn, R. M. (1991). The effects of microinjection of rhodamine-phallodin on mitosis and cytokinesis in early stage *Drosophila* embryos. *Exp. Cell Res.* **192**, 557-566.

Postner, M. A., Miller, K. G. and Weischaus, E. (1992). Maternal-effect mutations of the *sponge* locus affect cytoskeletal rearrangements in *Drosophila melanogaster* embryos. *J. Cell Biol.* **119**, 11205-1218

Rabinowitz, M. (1941). Studies on the cytology and early embryology of the egg of *Drosophila melanogaster*. *J. Morphol.* **69**, 1-49.

Rice, T. B. and Garen, A. (1975). Localized defects of blastoderm formation in maternal-effect mutants of *Drosophila*. *Dev. Biol.* **43**, 277-286.

Rose, L. S. and Wieschaus, E. (1992). The *Drosophila* cellularization gene *nullo* produces a blastoderm-specific transcript whose levels respond to the nucleocytoplasmic ratio. *Genes Dev.* **6**, 1255-1268.

Sandler, L. (1977). Evidence for a set of closely linked autosomal genes that interact with sex-chromosome heterochromatin in *Drosophila melanogaster*. *Genetics* **86**, 567-582.

Schupbach, T. and Wieschaus, E. (1986). Maternal-effect mutations altering the anterior-posterior pattern of the *Drosophila* embryo. *Roux's Arch. Dev. Biol.* **195**, 302-317.

Schupbach, T. and Wieschaus, E. (1989). Female sterile mutations on the second chromosome of Drosophila melanogaster. I. Maternal-effect mutations. *Genetics* **121**, 101-117.

Schweisguth, F., Lepesant, J. A. and Vincent, A. (1990). The serendipity alpha gene encodes a membrane associated protein required for the cellularization of the *Drosophila* embryo. *Genes Dev.* **4**, 922-931.

Schweisguth, F., Vincent, A. and Lepesant, J. A. (1991). Genetic analysis of the cellularization of the *Drosophila* embryo. *Biology of the Cell* **72**, 15-23.

Simpson, L. and Wieschaus, E. (1990). Zygotic activity of the nullo-locus is required to stabilize the actin-myosin network during cellularization in *Drosophila*. *Development* **110**, 851-863.

Sonnenblick, B. P. (1950). The early embryology of *Drosophila melanogaster*. In *Biology of Drosophila* (ed. M. Demerec), pp. 62-167. New York: John Wiley and Sons. Reprinted 1965, New York and London: Hafner.

St. Johnston, D., Beuchle, D. and Nusslein-Volhard, C. (1991). *staufen*, a gene required to localize maternal RNAs in the *Drosophila* egg. *Cell* **66**, 51-63.

Stafstrom, J. P. and Staehelin, L. A. (1984). Dynamics of the nuclear envelope and nuclear pore complexes during mitosis in the *Drosophila* embryo. *European Journal of Cell Biology* **34**, 179-189.

Sullivan, W. (1987). Independence of fushi tarazu expression with respect to cellular density in *Drosophila* embryos. *Nature* **327**, 164-167.

Sullivan, W., Minden, J. M. and Alberts, B. M. (1990). *daughterless-abo-like*, a *Drosophila* maternal-effect mutation that exhibits abnormal centrosome separation during the late blastoderm divisions. *Development* **110**, 311-323.

Szabad, J., Erdelyi, M., Hoffmann, G., Szidonya, J. and Wright, T. R. F. (1989). Isolation and characterization of dominant female sterile mutations of *Drosophila* melanogaster. II. Mutations on the second chromosome. *Genetics* **122**, 823-835.

Theurkauf, W. (1992). Behavior of structurally divergent alpha-tubulin isotypes during *Drosophila* embryogenesis: evidence for post-translational regulation of isotype abundance. *Dev. Biol.* **154**, 204-217.

Turner, R. R. and Mahowald, A. P. (1977). Scanning electron microscopy of *Drosophila* melanogaster embryogenesis. I. The structure of the egg envelope and the formation of the cellular blastoderm. *Dev. Biol.* **50**, 95-108.

Warn, R. M., Magrath, R. and Webb, S. (1984). Distribution of F-actin during cleavage of the *Drosophila* syncytial blastoderm. *J. Cell Biol.* **98**, 156-162.

Warn, R. M., Smith, L. and Warn, A. (1985). Three distinct distributions of F-actin occur during the divisions of polar surface caps to produce pole cells in *Drosophila* embryos. *J. Cell Biol.* **100**, 1010-1015.

Warn, R. M. and Warn, A. (1986). Microtubule arrays present during the syncytial and cellular blastoderm stages of the early *Drosophila* embryo. *Exp. Cell Res.* **163**, 201-210.

Warn, R. N., Flegg, L. and Warn, A. (1987). An investigation of microtubule organization and functions in living *Drosophila* embryos by injection of a fluorescently labeled antibody against tyrosinated tubulin. *J. Cell Biol.* **105**, 1721-1730.

Wieschaus, E. and Sweeton, D. (1988). Requirements of X-linked zygotic gene activity during cellularization of early *Drosophila* embryos. *Development* **104**, 483-493.

Zalokar, M., Audit, C. and Erk, I. (1975). Developmental defects of female-sterile mutants of *Drosophila melanogaster*. *Dev. Biol.* **47**, 419-432.

Zalokar, M. and Erk, I. (1976). Division and migration of nuclei during early embryogenesis of *Drosophila melanogaster*. *J. Microbiology Cell* **25**, 97-106.

(Accepted 4 May 1993)